

Article

## Studies on the Interactions of Copper and Zinc Ions with $\beta$ -Amyloid Peptides by a Surface Plasmon Resonance Biosensor

Fujun Yao <sup>1</sup>, Ruiping Zhang <sup>2,\*</sup>, He Tian <sup>2</sup> and Xiangjun Li <sup>1,\*</sup>

<sup>1</sup> College of Chemistry and Chemical Engineering, Graduate University, Chinese Academy of Sciences, Beijing, 100049, China; E-Mail: yaofuj09b@mails.gucas.ac.cn

<sup>2</sup> Institute of Materia Medica, Chinese Academy of Medical Sciences and Peking Union Medical College, Beijing 100050, China; E-Mail: tianhe@imm.ac.cn

\* Authors to whom correspondence should be addressed; E-Mails: rpzhang@imm.ac.cn (R.Z.); lixiangj@gucas.ac.cn (X.L.); Tel.: +86-10-6316-5218 (R.Z.); +86-10-8825-6336 (X.L.); Fax: +86-10-6316-5218 (R.Z.); +86-10-8825-6093 (X.L.).

Received: 18 July 2012; in revised form: 7 September 2012 / Accepted: 7 September 2012 /

Published: 19 September 2012

---

**Abstract:** The aggregation of  $\beta$ -amyloid peptide ( $A\beta$ ) into fibrils plays an important role in the pathogenesis of Alzheimer's disease (AD). Metal ions including copper and zinc are closely connected to the precipitation and toxicity of  $A\beta$ . In this study, a surface plasmon resonance (SPR) biosensor was constructed to investigate the interactions between  $A\beta$  and metal ions.  $A\beta$  peptide was immobilized on the SPR chip surface through a preformed alkanethiol self-assembled monolayer (SAM). Our observations indicate that the immobilized  $A\beta$  undergoes a conformational change upon exposure to the metal ions. A difference in metal binding affinity between  $A\beta_{1-28}$  and  $A\beta_{1-42}$  was also detected. The results suggest that SPR is an effective method to characterize the interactions between  $A\beta$  and metal ions.

**Keywords:** Alzheimer's disease;  $\beta$ -amyloid peptide; surface plasmon resonance; metal ions

---

### 1. Introduction

Alzheimer's disease (AD), which is characterized by irreversible and progressive neurodegeneration, is the dominant cause of dementia. The morphological hallmarks of AD are extracellular senile plaques

and intracellular neurofibrillary tangles. The aggregated  $\beta$ -amyloid peptide ( $A\beta$ ) containing 39–43 amino acid residues, which is generated from the amyloid precursor protein (APP) through the sequential cleavage by two enzymes,  $\beta$ -secretase and  $\gamma$ -secretase, is the principal component of the senile plaques. According to the amyloid cascade hypothesis, the aggregation of  $A\beta$  in AD leads to the formation of neurotoxic oligomers that are purportedly responsible for neuronal dysfunction and cell death [1]. Therefore, conditions that influence aggregation and the formation of oligomers are of great interest.

The aggregation of  $A\beta$  peptide is primarily affected by pH [2,3], peptide concentration [2], incubation time, membrane lipids [4] and temperature [5]. Moreover, a large body of evidence suggests that metal ions such as copper, zinc and iron may induce the aggregation of  $A\beta$  peptides, and these ligands may act as seeding factors in the formation of amyloid plaques [6–10]. In fact, elevated levels of zinc and copper have been found in amyloid plaques at concentrations reaching 1 mM and 400  $\mu$ M, respectively [11]. These metal ions bind at the N-terminus (amino acids 1–16) and influence aggregation behavior. However, experimental evidence has shown that these metal ions in complex with  $A\beta$  peptides may have opposite functions with Zn accelerating aggregation, while Cu can reduce or accelerate aggregation [12–14]. Furthermore, it has been proposed that copper and iron mediate the production of reactive oxygen species (ROS) and oxidative stress [15,16]. It has been reported that reactive oxygen species (ROS) such as  $H_2O_2$  are produced during the association of  $A\beta$  with  $Cu^{2+}$  through the reduction of  $Cu^{2+}$  to  $Cu^+$ , which mediates cell toxicity [17]. Therefore, intensive efforts have been made to study the primary interaction of  $A\beta$  peptide with metal ions.

Surface Plasmon resonance (SPR) spectroscopy is capable of detecting a mass or conformational change above a metal surface. At a specific angle, the absorption of incident light by a thin metal film causes a collective oscillation of electrons in the film that launches an evanescent wave into the dielectric layer adjacent to the metal film. The propagation of the evanescent wave decays exponentially away from the metal film and is thus significantly perturbed by the adsorption of a species on the metal film or changes in the adlayer structure. Due to the advantages of real-time, label-free and direct detection of molecules in various media, SPR has become a popular and powerful technique to study molecular interactions. In recent years, SPR has been successfully employed to study biomolecular interactions related to AD [18,19]. Various aspects of  $A\beta$  oligomerization, fibril formation and extension and  $A\beta$  interactions with biomolecules have been investigated by SPR [20,21]. A custom-built flow-injection (FI) SPR instrument equipped with a bicell detector was constructed in our lab and used to investigate the interactions between  $A\beta_{1-16}$  and metal ions [22]. Immobilization of monomeric  $A\beta$  was performed using a self-assembled monolayer (SAM) of 11-mercaptoundecanoic acid (MUA) and amino coupling chemistry. To further test the feasibility of this biosensor, the interactions between metal ions and  $A\beta_{1-28}$  or the actual senile plaque component,  $A\beta_{1-42}$ , were investigated.

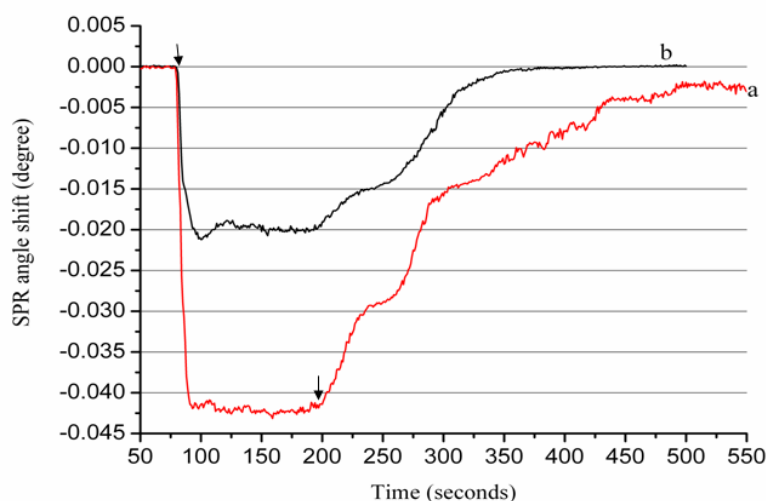
## 2. Results and Discussion

### 2.1. A $\beta$ Immobilization

The successful immobilization of the A $\beta$  peptide on the sensor chip surface was tested by injecting a Zn<sup>2+</sup> ion solution into the flow chamber and pumping it across the A $\beta$ -immobilized sensing surface. In our experiment, the sample loop volume is 20  $\mu$ L, the flowing rate is 10  $\mu$ L/min, so that the Zn<sup>2+</sup> ions start to flow onto the immobilized A $\beta$ <sub>1–28</sub> at about 80 s, the flowing of metal ions ends at about 200 s; the difference in the baseline SPR angles before and after the Zn<sup>2+</sup> ion solution injection (termed as the SPR dip shift  $\Delta\theta$ ) is approximately 0.00246° (Figure 1a), considering the sophisticated interaction between A $\beta$  peptide and metal ions, the detection of the SPR dip shift  $\Delta\theta$  is selected at 550 s.

To confirm that the net change is induced by the metal ions, we conducted a control experiment in which Zn<sup>2+</sup> ions flowed over an ethanolamine-blocked surface without the immobilization of A $\beta$  peptide. Figure 1b shows that the SPR signal returned to its baseline within a short time. Additionally, the recovery of the original baseline in curve b suggests that the blocking process is efficient because it has been reported that alkanethiol SAM containing carboxylic acid can be used for SPR measurements of heavy metal ions [23]. Furthermore, the conversion of the negatively charged carboxyl groups on the MUA SAM to neutral amide groups during the peptide immobilization and blocking process could reduce the undesirable electrostatic attraction to metal ions in solution.

**Figure 1.** The sensorgram of a 200  $\mu$ M Zn<sup>2+</sup> ion solution flowing over the surface plasmon resonance (SPR) sensor chip with (a) and without (b) immobilized  $\beta$ -amyloid peptides (A $\beta$ <sub>1–28</sub>) peptides. Arrows indicate Zn<sup>2+</sup> ions starting to flow onto immobilized A $\beta$ <sub>1–28</sub> and when the flowing of metal ions ends, respectively.

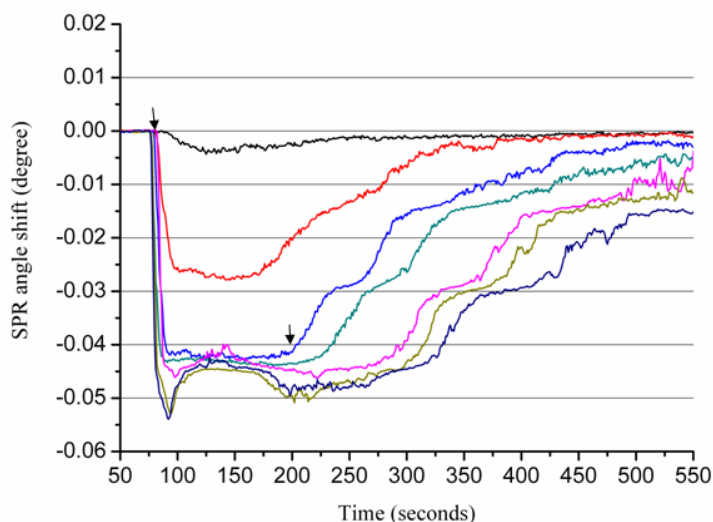


### 2.2. Real-Time Determination of A $\beta$ <sub>1–28</sub> Binding Zn<sup>2+</sup> and Cu<sup>2+</sup> by SPR

Figure 2 shows the sensorgrams of various Zn<sup>2+</sup> concentrations flowing over the A $\beta$ <sub>1–28</sub> sensor chip. In these experiments, EDTA (10 mM) was used to regenerate the surface. Therefore, a single chip can be used repeatedly for multiple samples. As shown in Figure 2, increasing Zn<sup>2+</sup> concentrations results in a greater SPR dip shift. When 600  $\mu$ M Zn<sup>2+</sup> flowed over the A $\beta$ <sub>1–28</sub>-covered SPR sensor, the metal

ions caused a net change of  $0.0075^\circ$ , which can be attributed to the binding of  $Zn^{2+}$  ions to  $A\beta_{1-28}$  resulting in conformational changes of the peptide molecules.

**Figure 2.** The sensorgrams for the interactions between  $Zn^{2+}$  ions and the  $A\beta_{1-28}$  peptides. Various concentrations (50, 100, 200, 300, 600, 700 and 800  $\mu M$ , from top to bottom) of  $Zn^{2+}$  ions were injected onto the  $A\beta_{1-28}$  sensorchip. Arrows indicate  $Zn^{2+}$  ions starting to flow onto immobilized  $A\beta_{1-28}$  and when the flowing of metal ions ends, respectively.



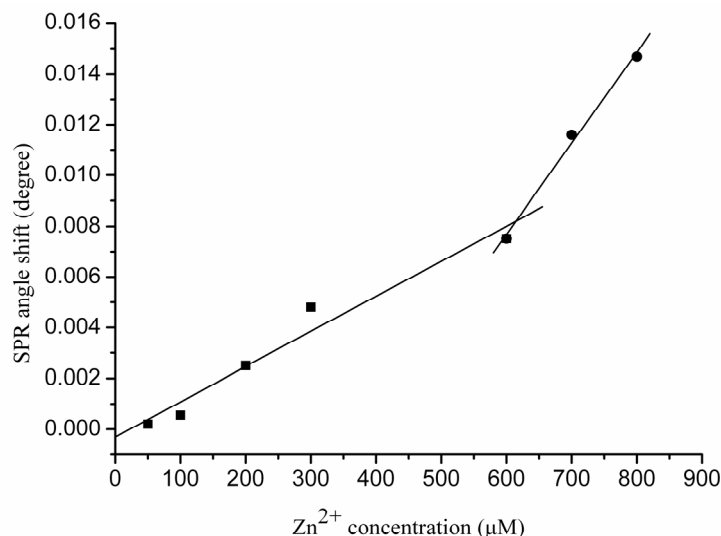
The SPR angle shift is directly correlated with the  $Zn^{2+}$  concentration ( $[Zn^{2+}]$ ). In Figure 3, the calibration curve generated from the sensor response to a series of different  $Zn^{2+}$  concentrations is shown. The calibration curve contains two regions; the first is from 50 to 300  $\mu M$ , and the second from 600 to 800  $\mu M$ . Linear regression analysis of both regions yielded the following equations:

$$\Delta\theta = -3.07 \times 10^{-4} + 1.39 \times 10^{-5} [Zn^{2+}] \quad R^2 = 0.95 \text{ (region 1)} \quad (1)$$

$$\Delta\theta = -1.39 \times 10^{-2} + 3.59 \times 10^{-5} [Zn^{2+}] \quad R^2 = 0.99 \text{ (region 2)} \quad (2)$$

The slope of the linear regression in the second region is higher than that in the first region, which reveals that the SPR angle shift elicited by  $Zn^{2+}$  ions is greater with increasing  $Zn^{2+}$  ion concentration. These results suggest that the  $Zn^{2+}$ -induced  $A\beta_{1-28}$  conformation change is concentration dependent. This finding is in agreement with a previous report indicating that  $A\beta$  undergoes a conformational change from a random coil to a regular secondary structure in the presence of  $Zn^{2+}$  ions and forms stable 1:1 and 1:2 (peptide/zinc) complexes [8]. A possible explanation for this phenomenon is that the  $A\beta_{1-28}$  binds  $Zn^{2+}$  intramolecularly at low concentrations. When the  $Zn^{2+}$  ion concentration is sufficiently high, the excess  $Zn^{2+}$  ions may begin to bind with  $A\beta_{1-28}$  intermolecularly, and the  $Zn^{2+}$  ions behave like a bridge connecting two adjacent  $A\beta_{1-28}$  molecules. Our finding is supported by previous studies that have shown that  $Zn^{2+}$  can coordinate to  $A\beta$  in an intra- and inter-peptide mode [24–26].

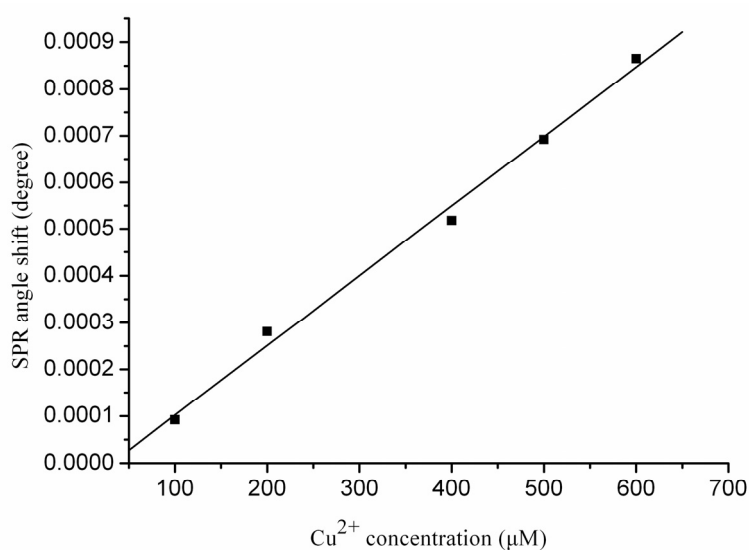
**Figure 3.** Calibration curves for the interactions between various  $Zn^{2+}$  concentrations with  $A\beta_{1-28}$ . Each value represents the mean  $\pm$  standard deviation of three separate injections.



A similar trend was not found for the interactions between  $Cu^{2+}$  and  $A\beta_{1-28}$ . The calibration curve depicted in Figure 4 only contains one linear region ranging from 100 to 600  $\mu M$ . The linear regression equation with a correlation coefficient of  $R^2 = 0.99$  suggests a linear relationship between the SPR angle shift and the  $Cu^{2+}$  concentration.

$$\Delta\theta = -4.67 \times 10^{-5} + 1.49 \times 10^{-6} [Cu^{2+}] R^2 = 0.99 \quad (3)$$

**Figure 4.** The calibration curve for the interactions between various  $Cu^{2+}$  concentrations with  $A\beta_{1-28}$ . Each value represents the mean  $\pm$  standard deviation of three separate injections.



Compared with  $Zn^{2+}$ - $A\beta$  complexes having stoichiometry ranging from 1:1 to 3:1 [27–29], most studies have demonstrated that the  $A\beta$ -peptide forms a 1:1 complex with  $Cu^{2+}$  [25,30,31]. NMR studies have demonstrated that  $A\beta_{1-28}$  forms a 1:1 complex with the  $Cu^{2+}$  ion via histidine

residues [30]. We interpret these results to different coordination modes. Unlike  $Zn^{2+}$ , which can bind to A $\beta$  in an intra- and inter-peptide coordination mode,  $Cu^{2+}$  is primarily involved in intra-peptide binding in a fairly closed structure that protects the metal from further interactions. In addition, it has been reported that under physiological conditions, the coordination of the  $Cu^{2+}$  equivalent to the A $\beta$  peptides leads to a mononuclear complex  $Cu_1(A\beta)_1$  and is unlikely to form a  $Cu_2(A\beta)_1$  complex [32].

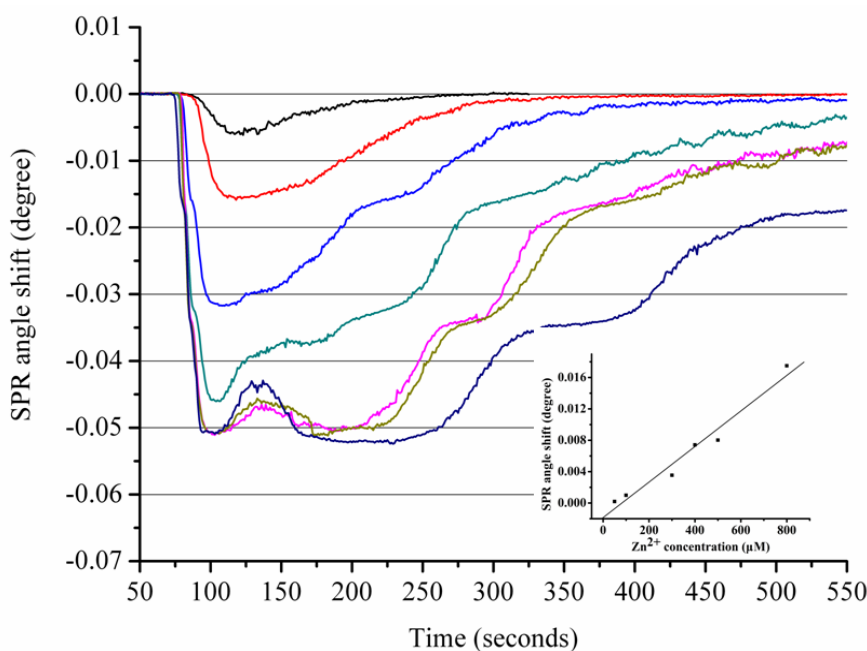
### 2.3. Real-Time Determination of $A\beta_{1-42}$ Binding to $Zn^{2+}$ and $Cu^{2+}$ by SPR

A $\beta_{1-40}$  and A $\beta_{1-42}$  are the most prevalent *in vivo* A $\beta$  forms. In particular, A $\beta_{1-42}$  has a high propensity to self-assemble and deposit in senile plaques and is highly toxic to neurons [33]. While great progress has been achieved on the coordination chemistry of  $Zn^{2+}$  and  $Cu^{2+}$  with truncated A $\beta_{1-16}$  and A $\beta_{1-28}$ , it is important to understand whether these peptides, which are missing a large part of the hydrophobic C-terminal residues, coordinate metal ions differently than the full-length peptides. Therefore, to better understand the mechanisms of AD, we continued to study the interactions of  $Zn^{2+}$  and  $Cu^{2+}$  with A $\beta_{1-42}$  using the FI-SPR biosensor.

Figure 5 depicts SPR sensorgrams obtained from the sensor response to various  $Zn^{2+}$  concentrations. In contrast to the calibration curve of the  $Zn^{2+}$  interactions with A $\beta_{1-28}$  that contains two regions, the calibration plot of the Zn interactions with A $\beta_{1-42}$  only contains one region; the linear regression equation is as follows:

$$\Delta\theta = -1.86 \times 10^{-3} + 2.27 \times 10^{-5} [Zn^{2+}] R^2 = 0.96 \quad (4)$$

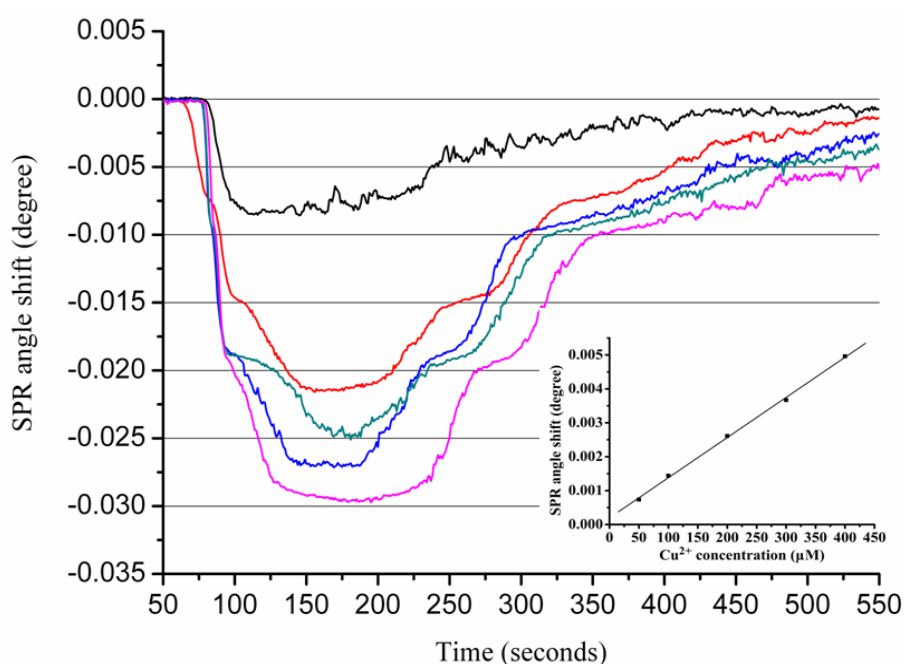
**Figure 5.** The sensorgram for the interactions between  $Zn^{2+}$  ions and A $\beta_{1-42}$ . Various concentrations (50, 100, 300, 400, 500 and 800  $\mu$ M, from top to bottom) of  $Zn^{2+}$  ions were injected onto the A $\beta_{1-42}$  sensorchip. The inset shows the calibration curve for the interactions between various concentrations of  $Zn^{2+}$  with A $\beta_{1-42}$ . Each value represents the mean  $\pm$  standard deviation of three separate injections. Arrows indicate  $Zn^{2+}$  ions starting to flow onto immobilized A $\beta_{1-42}$  and when the flow of metal ions ends, respectively.



A $\beta_{1-42}$  peptides have 14 additional residues in the hydrophobic tail compared to A $\beta_{1-28}$ , which makes A $\beta_{1-42}$  more prone to aggregation than the truncated A $\beta_{1-28}$ . A possible explanation for the decreased stoichiometric binding of A $\beta_{1-42}$  compared to A $\beta_{1-28}$  may be the interference of the hydrophobic tail in A $\beta_{1-42}$  with the Zn<sup>2+</sup> binding site. Our data are in agreement with a previous report indicating that Zn and Cu form a monomeric complex with A $\beta_{1-42}$  [34].

Similar results were obtained for the Cu-A $\beta_{1-42}$  interaction. As shown in Figure 6, the SPR angle shift increased with an increase of Cu<sup>2+</sup> bound to the A $\beta_{1-42}$ -immobilized sensor chip. The calibration curve generated from the sensor exposed to different concentrations of Cu<sup>2+</sup> is shown in the Figure 6 inset. A strong correlation coefficient ( $R^2 = 0.99$ ) was obtained for the linear regression equation calculated using Cu<sup>2+</sup> concentrations ranging from 50 to 400  $\mu$ M.

**Figure 6.** The sensorgram for the interactions between Cu<sup>2+</sup> ions and A $\beta_{1-42}$ . Various concentrations (50, 100, 200, 300, and 400  $\mu$ M, from top to bottom) of Cu<sup>2+</sup> ions were injected onto the A $\beta_{1-42}$  sensorchip. The inset shows the calibration curve for the interactions between various concentrations of Cu<sup>2+</sup> with A $\beta_{1-42}$ . Each value represents the mean  $\pm$  standard deviation of three separate injections. Arrows indicate Cu<sup>2+</sup> ions starting to flow onto immobilized A $\beta_{1-28}$  and when the flow of metal ions ends, respectively.



### 3. Experimental Section

#### 3.1. Chemicals

Human amyloid- $\beta$  peptide (1–28) (A $\beta_{1-28}$ ) and human amyloid- $\beta$  peptide (1–42) (A $\beta_{1-42}$ ) were obtained from GL Biochem Ltd. (Shanghai, China). 1-(3-Dimethylaminopropyl)-3-ethylcarbodiimide hydrochloride (EDC), *N*-hydroxysulfosuccinimide (NHS), 11-mercaptoundecanoic acid (MUA), ARC-grade dimethyl sulfoxide (DMSO, 99%) and ethanolamine were purchased from J & K Chemical Ltd. K<sub>2</sub>HPO<sub>4</sub>·3H<sub>2</sub>O, KH<sub>2</sub>PO<sub>4</sub>, NaCl, ZnCl<sub>2</sub> and CuCl<sub>2</sub> were all of AR grade and purchased from Beijing Chemical Reagent Co. (Beijing, China). Water with a resistivity of 18.25 M $\Omega$ ·cm<sup>-1</sup> was

collected from a Millipore Simplicity 185 system. EDC (0.4 M) and NHS (0.1 M) were prepared in a pH 7.4 PBS buffer (10.0 mM  $K_2HPO_4 \cdot 3H_2O$  and  $KH_2PO_4$  prepared in 1 mM NaCl). MUA (4 mM) was prepared in pure ethanol. Stock solutions of 2.0 mM  $ZnCl_2$  and  $CuCl_2$  were prepared in water and then diluted to the desired concentrations.

### 3.2. Preparation of Fresh A $\beta$ Solution

Uniform and nonaggregated monomeric A $\beta_{1-28}$  and A $\beta_{1-42}$  peptides were prepared as previously described [35]. Briefly, 0.1 mM of the peptide was dissolved in DMSO, which disrupts the  $\beta$ -sheet structure and renders A $\beta$  monomeric [36]. The freshly dissolved monomeric A $\beta$  was diluted with PBS buffer (pH 7.4) to a concentration of 10  $\mu$ M.

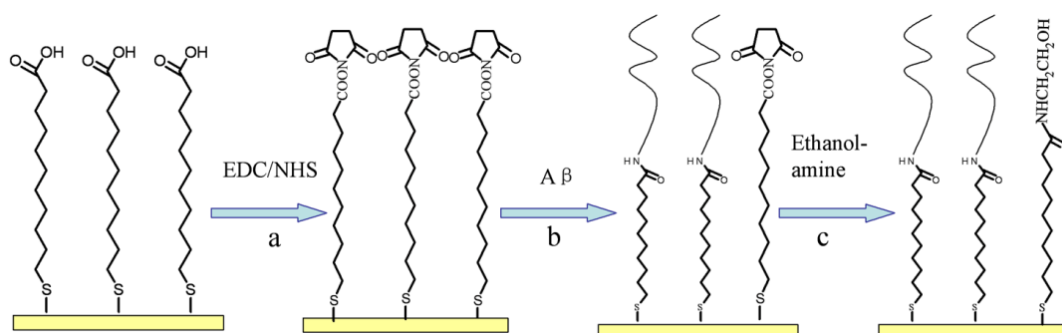
### 3.3. Gold Film Preparation

BK7 glass cover slides (Fisher) were cleaned with a piranha solution of 70% concentrated  $H_2SO_4$  and 30%  $H_2O_2$  (7:3, v/v) at 80 °C for 30 min. Upon cooling to room temperature, the glass slides were rinsed thoroughly with deionized water. After drying with  $N_2$ , each glass slide was coated with a 2 nm chromium layer and then covered with 50 nm of gold film using a sputter coater (Model 108, Kert J. Lester Inc., Clariton, PA, USA).

### 3.4. A $\beta$ Peptide Immobilization

A $\beta$  peptide immobilization was achieved using covalent bonding mediated by a chemical reaction. The *N*-terminus of the A $\beta$  peptide was reacted with the functional group of the SAM of MUA on the surface of the Au film (as depicted in Figure 7). Briefly, the MUA gold chip was treated with a mixture of 0.4 M EDC and 0.1 M NHS (1:1) for 3 h to ensure that the carboxyl group of the SAM reacted fully with the EDC and NHS. Then, a freshly prepared 10  $\mu$ M A $\beta$  solution in PBS (pH 7.4) was reacted with the NHS-activated surface for 2 h. Finally, ethanolamine (1 M, pH 8.5) was used to block the remaining activated surface groups. The resulting film was either used immediately or stored at 4 °C for future use.

**Figure 7.** The procedure for the immobilization of A $\beta$ . (a) The self-assembled monolayer (SAM) of MUA surface was activated with standard amine coupling chemistry using EDC/NHS; (b) The activated surface was covered with a fresh A $\beta$  solution to form a bond between the amine group on the peptide and the carboxylic group on the MUA surface; (c) The remaining activated surface groups were blocked using ethanolamine.



### 3.5. SPR Apparatus

SPR measurements were conducted with a custom-built flow injection-SPR equipped with a bicell detector as previously described [22]. The SPR instrument recorded the reflected light on two photodetectors (A and B). The differential ( $A - B$ ) and sum ( $A + B$ ) signals were then detected by a PCI-1371 interface card (Advantech, Taiwan) controlled by the Labview program. The resonance angles from the biosensor were measured by the division of the differential and sum signals,  $(A - B)/(A + B)$ . The inlet of the flow cell was connected to a six-port valve. For each measurement, the sample solution was injected into a 20- $\mu$ L loop with a microsyringe (Hamilton) and subsequently delivered to the flow cell at a flow rate of 10  $\mu$ L/min, using a syringe pump (KDS100, KD Scientific Inc., Holliston, MA, USA).

## 4. Conclusions

In the present study, a SPR-based analytical method was used to investigate the interactions between A $\beta$  peptides and metal ions. The coordination of metal ions with the truncated A $\beta$ <sub>1–28</sub> and the full-length A $\beta$ <sub>1–42</sub> were compared. The conformational transition of A $\beta$  induced by metal ion binding can be readily detected by this highly sensitive FI-SPR sensor equipped with a bicell detector. At physiological pH, Zn<sup>2+</sup> demonstrates different binding affinity for A $\beta$ <sub>1–28</sub> and A $\beta$ <sub>1–42</sub>, while Cu<sup>2+</sup> exhibits similar interactions with both A $\beta$  peptides. The interactions between Zn<sup>2+</sup> and the A $\beta$ -peptides in an intra- and inter-molecular mode have been previously validated. These studies complement other analytical methods and should help elucidate the role of metal ions during A $\beta$  aggregation.

## Acknowledgments

This work was supported by the National Natural Science Foundation of China (21145006), Scientific Research Foundation for the Returned Overseas Chinese Scholars, State Education Ministry and Beijing Municipal Natural Science Foundation (2113046).

## References

1. Roychaudhuri, R.; Yang, M.; Hoshi, M.M.; Teplow, D.B. Amyloid  $\beta$ -protein assembly and Alzheimer disease. *J. Biol. Chem.* **2009**, *284*, 4749–4753.
2. Burdick, D.; Soreghan, B.; Kwon, M.; Kosmoski, J.; Knauer, M.; Henschen, A.; Yates, J.; Cotman, C.; Glabe, C. Assembly and aggregation properties of synthetic Alzheimer's A4/ $\beta$  amyloid peptide analogs. *J. Biol. Chem.* **1992**, *267*, 546–554.
3. Fraser, P.E.; Nguyen, J.T.; Surewicz, W.K.; Kirschner, D.A. pH-dependent structural transitions of Alzheimer amyloid peptides. *Biophys. J.* **1991**, *60*, 1190–1201.
4. McLaurin, J.; Franklin, T.; Chakrabartty, A.; Fraser, P.E. Phosphatidylinositol and inositol involvement in Alzheimer amyloid- $\beta$  fibril growth and arrest. *J. Mol. Biol.* **1998**, *278*, 183–194.
5. Yamaguchi, T.; Matsuzaki, K.; Hoshino, M. Transient formation of intermediate conformational states of amyloid- $\beta$  peptide revealed by heteronuclear magnetic resonance spectroscopy. *FEBS Lett.* **2011**, *585*, 1097–1102.

6. Bush, A.I.; Pettingell, W.H.; Multhaup, G.; d Paradis, M.; Vonsattel, J.P.; Gusella, J.F.; Beyreuther, K.; Masters, C.L.; Tanzi, R.E. Rapid induction of Alzheimer A $\beta$  amyloid formation by zinc. *Science* **1994**, *265*, 1464–1467.
7. Miura, T.; Suzuki, K.; Kohata, N.; Takeuchi, H. Metal binding modes of Alzheimer's amyloid  $\beta$ -peptide in insoluble aggregates and soluble complexes. *Biochemistry* **2000**, *39*, 7024–7031.
8. Kozin, S.A.; Zirah, S.; Rebuffat, S.; Hoa, G.H.; Debey, P. Zinc binding to Alzheimer's A $\beta$ (1–16) peptide results in stable soluble complex. *Biochem. Biophys. Res. Commun.* **2001**, *285*, 959–964.
9. Chen, T.; Wang, X.; He, Y.; Zhang, C.; Wu, Z.; Liao, K.; Wang, J.; Guo, Z. Effects of cyclen and cyclam on zinc(II)- and copper(II)-induced amyloid  $\beta$ -peptide aggregation and neurotoxicity. *Inorg. Chem.* **2009**, *48*, 5801–5809.
10. Sarell, C.J.; Syme, C.D.; Rigby, S.E.; Viles, J.H. Copper(II) binding to amyloid-beta fibrils of Alzheimer's disease reveals a picomolar affinity: Stoichiometry and coordination geometry are independent of A $\beta$  oligomeric form. *Biochemistry* **2009**, *48*, 4388–4402.
11. Lovell, M.A.; Robertson, J.D.; Teesdale, W.J.; Campbell, J.L.; Markesbery, W.R. Copper, iron and zinc in Alzheimer's disease senile plaques. *J. Neurol. Sci.* **1998**, *158*, 47–52.
12. Atwood, C.S.; Moir, R.D.; Huang, X.; Scarpa, R.C.; Bacarra, N.M.; Romano, D.M.; Hartshorn, M.A.; Tanzi, R.E.; Bush, A.I. Dramatic aggregation of Alzheimer A $\beta$  by Cu(II) is induced by conditions representing physiological acidosis. *J. Biol. Chem.* **1998**, *273*, 12817–12826.
13. Zou, J.; Kajita, K.; Sugimoto, N. Cu<sup>2+</sup> inhibits the aggregation of amyloid  $\beta$ -peptide(1–42) *in vitro*. *Angew. Chem. Int. Ed.* **2001**, *40*, 2274–2277.
14. Raman, B.; Ban, T.; Yamaguchi, K.; Sakai, M.; Kawai, T.; Naiki, H.; Goto, Y. Metal ion-dependent effects of clioquinol on the fibril growth of an amyloid  $\beta$  peptide. *J. Biol. Chem.* **2005**, *280*, 16157–16162.
15. Huang, X.; Atwood, C.S.; Hartshorn, M.A.; Multhaup, G.; Goldstein, L.E.; Scarpa, R.C.; Cuajungco, M.P.; Gray, D.N.; Lim, J.; Moir, R.D.; *et al.* The A $\beta$  peptide of Alzheimer's disease directly produces hydrogen peroxide through metal ion reduction. *Biochemistry* **1999**, *38*, 7609–7616.
16. Kowalik-Jankowska, T.; Ruta, M.; Wisniewska, K.; Lankiewicz, L.; Dyba, M. Products of Cu(II)-catalyzed oxidation in the presence of hydrogen peroxide of the 1–10, 1–16 fragments of human and mouse  $\beta$ -amyloid peptide. *J. Inorg. Biochem.* **2004**, *98*, 940–950.
17. Ali, F.E.; Separovic, F.; Barrow, C.J.; Cherny, R.A.; Fraser, F.; Bush, A.I.; Masters, C.L.; Barnham, K.J. Methionine regulates copper/hydrogen peroxide oxidation products of A $\beta$ . *J. Pept. Sci.* **2005**, *11*, 353–360.
18. Ryu, J.; Joung, H.A.; Kim, M.G.; Park, C.B. Surface plasmon resonance analysis of Alzheimer's  $\beta$ -amyloid aggregation on a solid surface: from monomers to fully-grown fibrils. *Anal. Chem.* **2008**, *80*, 2400–2407.
19. Xia, N.; Liu, L.; Harrington, M.G.; Wang, J.; Zhou, F. Regenerable and simultaneous surface plasmon resonance detection of A $\beta$ (1–40) and A $\beta$ (1–42) peptides in cerebrospinal fluids with signal amplification by streptavidin conjugated to an *N*-terminus-specific antibody. *Anal. Chem.* **2010**, *82*, 10151–10157.
20. Aguilar, M.I.; Small, D.H. Surface plasmon resonance for the analysis of  $\beta$ -amyloid interactions and fibril formation in Alzheimer's disease research. *Neurotox. Res.* **2005**, *7*, 17–27.

21. Krazinski, B.E.; Radecki, J.; Radecka, H. Surface plasmon resonance based biosensors for exploring the influence of alkaloids on aggregation of amyloid- $\beta$  peptide. *Sensors* **2011**, *11*, 4030–4042.
22. Yao, F.; He, J.; Li, X.; Zou, H.; Yuan, Z. Studies of interaction of copper and zinc ions with Alzheimer's A $\beta$ (1–16) using surface plasmon resonance spectrometer. *Sens. Actuators B* **2012**, *161*, 886–891.
23. Saber, R.; Piskin, E. Investigation of complexation of immobilized metallothionein with Zn(II) and Cd(II) ions using piezoelectric crystals. *Biosens. Bioelectron.* **2003**, *18*, 1039–1046.
24. Stellato, F.; Menestrina, G.; Serra, M.D.; Potrich, C.; Tomazzolli, R.; Meyer-Klaucke, W.; Morante, S. Metal binding in amyloid  $\beta$ -peptides shows intra- and inter-peptide coordination modes. *Eur. Biophys. J.* **2006**, *35*, 340–351.
25. Syme, C.D.; Viles, J.H. Solution  $^1\text{H}$  NMR investigation of Zn $^{2+}$  and Cd $^{2+}$  binding to amyloid- $\beta$  peptide (A $\beta$ ) of Alzheimer's disease. *Biochim. Biophys. Acta* **2006**, *1764*, 246–256.
26. Miller, Y.; Ma, B.; Nussinov, R. Zinc ions promote Alzheimer A $\beta$  aggregation via population shift of polymorphic states. *Proc. Natl. Acad. Sci. USA* **2010**, *107*, 9490–9495.
27. Clements, A.; Allsop, D.; Walsh, D.M.; Williams, C.H. Aggregation and metal-binding properties of mutant forms of the amyloid A $\beta$  peptide of Alzheimer's disease. *J. Neurochem.* **1996**, *66*, 740–747.
28. Atwood, C.S.; Scarpa, R.C.; Huang, X.; Moir, R.D.; Jones, W.D.; Fairlie, D.P.; Tanzi, R.E.; Bush, A.I. Characterization of copper interactions with alzheimer amyloid  $\beta$  peptides: Identification of an attomolar-affinity copper binding site on amyloid  $\beta$ 1-42. *J. Neurochem.* **2000**, *75*, 1219–1233.
29. Damante, C.A.; Osz, K.; Nagy, Z.; Pappalardo, G.; Grasso, G.; Impellizzeri, G.; Rizzarelli, E.; Sovago, I. Metal loading capacity of A $\beta$  N-terminus: A combined potentiometric and spectroscopic study of zinc(II) complexes with A $\beta$ (1–16), its short or mutated peptide fragments and its polyethylene glycol-ylated analogue. *Inorg. Chem.* **2009**, *48*, 10405–10415.
30. Karr, J.W.; Akintoye, H.; Kaupp, L.J.; Szalai, V.A. N-Terminal deletions modify the Cu $^{2+}$  binding site in amyloid- $\beta$ . *Biochemistry* **2005**, *44*, 5478–5487.
31. Tōugu, V.; Karafin, A.; Palumaa, P. Binding of zinc(II) and copper(II) to the full-length Alzheimer's amyloid- $\beta$  peptide. *J. Neurochem.* **2008**, *104*, 1249–1259.
32. Faller, P.; Hureau, C. Bioinorganic chemistry of copper and zinc ions coordinated to amyloid- $\beta$  peptide. *Dalton Trans.* **2009**, *7*, 1080–1094.
33. Findeis, M.A. The role of amyloid  $\beta$  peptide 42 in Alzheimer's disease. *Pharmacol. Ther.* **2007**, *116*, 266–286.
34. Walsh, D.M.; Lomakin, A.; Benedek, G.B.; Condron, M.M.; Teplow, D.B. Amyloid  $\beta$ -protein fibrillogenesis. Detection of a protofibrillar intermediate. *J. Biol. Chem.* **1997**, *272*, 22364–22372.
35. Hu, W.P.; Chang, G.L.; Chen, S.J.; Kuo, Y.M. Kinetic analysis of  $\beta$ -amyloid peptide aggregation induced by metal ions based on surface plasmon resonance biosensing. *J. Neurosci. Meth.* **2006**, *154*, 190–197.

36. Kremer, J.J.; Pallitto, M.M.; Sklansky, D.J.; Murphy, R.M. Correlation of  $\beta$ -amyloid aggregate size and hydrophobicity with decreased bilayer fluidity of model membranes. *Biochemistry* **2000**, *39*, 10309–10318.

© 2012 by the authors; licensee MDPI, Basel, Switzerland. This article is an open access article distributed under the terms and conditions of the Creative Commons Attribution license (<http://creativecommons.org/licenses/by/3.0/>).